Comparison of the Subunit Compositions of the PSI−LHCI Supercomplex and the LHCI in the Green Alga *Chlamydomonas reinhardtii*†

Yuichiro Takahashi,*,‡ Taka-aki Yasui,‡ Einar J. Stauber,§ and Michael Hippler§

Department of Biology, Faculty of Science, Okayama University, 3-1-1, Tsushima-naka, Okayama, 700-8530, Japan, and Lehrstuhl für Pflanzenphysiologie, Friedrich-Schiller-Universität Jena, Dornburger Str. 159, 07743 Jena, Germany

Received November 6, 2003; Revised Manuscript Received March 25, 2004

ABSTRACT: Although the light-harvesting chlorophyll protein complex I (LHCI) of photosystem I (PSI) is intimately associated with the PSI core complex and forms the PSI−LHCI supercomplex, the LHCI is normally synthesized in PSI-deficient mutants. In this paper, we compared the subunit compositions of the PSI−LHCI supercomplex and the LHCI by immunoblot analysis and two-dimensional gel electrophoresis combined with mass spectrometry. The PSI−LHCI supercomplex and the LHCI were purified by sucrose density gradient centrifugation and (diethylamino)ethyl column chromatography from *n*-dodecyl-*β*-D-maltoside-solubilized thylakoids of the wild-type and Δ*psaB* mutant of the green alga *Chlamydomonas reinhardtii*. The PSI−LHCI supercomplex contained all of the nine Lhca polypeptides (Lhca1−9) that are detected in wild-type thylakoids. In contrast, the LHCI retained only six Lhca polypeptides, whereas Lhca3 and two minor polypeptides, Lhca2 and Lhca9, were lost during the purification procedure. Sucrose density gradient centrifugation showed that the purified LHCI retains an oligomeric structure with an apparent molecular mass of 300−400 kDa. We therefore concluded that Lhca2, Lhca3, and Lhca9 are not required for the stable oligomeric structure of the LHCI and that the association of these polypeptides in the LHCI is stabilized by the presence of the PSI core complex. Finally, we discuss the possible localization and function of Lhca polypeptides in the LHCI.

Light energy used to drive photosynthetic electron transport is absorbed by antenna pigments located in the thylakoid membranes. In higher plants and green algae, antenna pigments reside in core and accessory antenna systems. The core antenna system is fused with reaction center proteins such as the PsaA/PsaB heterodimer in photosystem I (PSI)[1] or is intimately associated with the reaction center complex like CP43 and CP47 in photosystem II (PSII). The accessory antenna systems are called the light-harvesting chlorophyll a/b complexes (LHC). LHCI is functionally related to PSI as is LHCII to PSII. It is known that LHCI is tightly associated with the PSI core complex, and thus the PSI−LHCI supercomplex is easily purified after solubilizing thylakoids with nonionic detergents (*1*). On the contrary, LHCII is loosely associated with the PSII core complex, and thus the PSII−LHCII supercomplex can be isolated only under mild conditions (*2*).

LHCI forms an oligomer and consists of several distinct Lhca polypeptides (*3*). Two types of LHCI have been isolated from higher plants: LHCI-680, which consists of Lhca2 and Lhca3 and emits 77 K fluorescence peaking at 680 nm, and LHCI-730, which consists of Lhca1 and Lhca4 and emits fluorescence at 730 nm (*4*). The number of Lhca polypeptides present in the PSI−LHCI supercomplex currently remains controversial. The three-dimensional structure of the PSI−LHCI supercomplex, as characterized by single particle analysis with electron microscopy, suggests that 8−14 Lhca polypeptides are present (*5*−*7*). Because the Lhca polypeptide is estimated to bind 10−12 chlorophyll molecules, there must be 100 or more chlorophyll molecules bound to LHCI in the supercomplex (*8*). The structure of the PSI−LHCI supercomplex also suggests that Lhca polypeptides form a half-ring structure and are bound at one side of the PSI core complex (*5*). Recently, the crystal structure of plant PSI−LHCI supercomplex has been determined at a 4.4-Å resolution (*9*). The structure revealed that the supercomplex contains only 4 Lhca polypeptides. It is of interest that the PSI−LHCI supercomplex from *Chlamydomonas reinhardtii* is significantly larger than the corresponding complex in spinach (*6*). However, the assignment and function of individual Lhca polypeptides in the PSI−LHCI supercomplex remain to be elucidated.

The LHCI complex of *C. reinhardtii* was initially identified as CPO (chlorophyll protein O) by nondenaturing lithium dodecyl sulfate polyacrylamide gel electrophoresis (*10*). The relative electrophoretic mobility on the gel was lower than that of CPI (PSI reaction center complex), suggesting that CPO forms a high molecular weight complex. Because the structure of the PSI−LHCI supercomplex appears similar in *C. reinhardtii* and higher plants, the oligomeric structure

† This research was supported by a grant in aid for General Research (C) (2) (15570037) to Y.T. and by grants from the Deutsche Forschungsgemeinschaft and the Freistaat Thüringen to M.H.

* To whom correspondence should be addressed. Tel: +81-86-251-7861. Fax: +81-86-251-7876. E-mail: taka@cc.okayama-u.ac.jp.

‡ Okayama University.

§ Friedrich-Schiller-Universität Jena.

[1] Abbreviations: Chl, chlorophyll; CPO, chlorophyll protein O; DM, *n*-dodecyl-*β*-D-maltoside; LHCI, light-harvesting complex I; LHCII, light-harvesting complex II; PSI, photosystem I; PSII, photosystem II; 2DE, two-dimensional electrophoresis.

10.1021/bi035988z CCC: $27.50
Published on Web 05/26/2004

of *C. reinhardtii* LHCI is rather stable compared with that of higher plants. It was also found that CPO accumulates normally in the PSI-deficient mutant (*10*). This indicates that assembly of the LHCI is independent of the PSI complex and that the oligomeric form of the LHCI accumulates stably in vivo even in the absence of the PSI core complex. Two types of the LHCI, LHCI-680 and LHCI-705, which emit 77 K fluorescence at 685 and 705 nm, respectively, have been isolated from the PSI−LHCI supercomplex of *C. reinhardtii*. In contrast to LHCI-680 and LHCI-730 in higher plants, the polypeptide composition of LHCI-680 and LHCI-705 is very similar (*3*). Detailed biochemical analyses revealed that there are nine distinct Lhca polypeptides in *C. reinhardtii* (*11*).

In the present paper, we purified the PSI−LHCI supercomplex and the LHCI from *C. reinhardtii* wild-type and Δ*psaB* cells and compared the polypeptide compositions by SDS−PAGE and Western blotting. In addition, to compare the polypeptides in the PSI−LHCI supercomplex and LHCI at high resolution and sensitivity, we employed two-dimensional gel electrophoresis (2DE) combined with tandem mass spectrometry (MS/MS). We found that the LHCI from the Δ*psaB* mutant still contained most of the major Lhca polypeptides found in the PSI−LHCI supercomplex. Immunoblotting, however, revealed that Lhca3 (p14.1) is lost during the preparation of the LHCI from Δ*psaB* cells. The 2DE identified two additional minor polypeptides that were decreased in the purified LHCI. In conclusion, the association of these Lhca proteins with the LHCI is stabilized by the presence of the PSI core complex, but the presence of these polypeptides is not required for stabilizing the oligomeric structure of the LHCI.

EXPERIMENTAL PROCEDURES

Strains and Growth Conditions. In these studies, we used the *C. reinhardtii* wild-type strain 137C and the *psaB*-deficient mutant (Δ*psaB*). Cells were grown to mid-log phase [$(2-5) \times 10^6$ cells mL^{-1}] in a Tris-acetate-phosphate (TAP) medium at 25 °C.

Purification of Chlorophyll−Protein Complexes. Thylakoid membranes were purified by discontinuous sucrose density gradient centrifugation as described previously (*12*). The thylakoid membranes (0.8 mg Chl mL^{-1}) were solubilized with 0.8% (w/v) *n*-dodecyl-*β*-D-maltoside (DM), and the resulting extracts were fractionated by sucrose density gradient centrifugation as described previously (*13*). The sucrose gradient contained a linear concentration of sucrose from 0.1 to 1.3 M in 5 mM Tricine-NaOH at pH 8.0 and 0.05% DM, and centrifugation was carried out at 141000*g* (SW28, Beckman) at 4 °C for 24 h. The chlorophyll−protein complexes were further separated by column chromatography on (diethylamino)ethyl (DEAE) Toyopearl 650S (Tosoh, Tokyo, Japan). Fractions were eluted with a linear gradient of NaCl (25−175 mM) in 50 mM Tris-HCl at pH 8.0 and 0.05% DM. Chlorophyll concentrations were determined as described in ref *14*.

Western Blotting. Polypeptides were solubilized with 2% SDS and 0.1 M dithiothreitol at 100 °C for 1 min and separated by SDS−PAGE according to ref *15*. D1 was resolved by urea−SDS−PAGE as described in ref *13*. To improve the separation of LHCI polypeptides around 20−30 kDa, an SDS−PAGE system with a high Tris buffer and gradient acrylamide concentration (15−22.5%) was used in the resolving gel (*16*). Separated polypeptides were electrophoretically transferred to nitrocellulose filters and then probed with specific polyclonal antibodies. The signals were visualized by enhanced chemiluminescence.

2DE and MS. The 2DE was performed as described in ref *17*, and mass spectrometric analyses were conducted as described in ref *11*.

Measurement of Fluorescence Emission Spectra. Fluorescence emission spectra were measured at 77 K with a Hitachi fluorescence spectrophotometer F-4500. Samples were excited with an actinic light at 430 nm.

RESULTS

Purification of PSI−LHCI Supercomplex from Wild-Type Cells. LHCI is tightly bound to the PSI core complex so that the PSI−LHCI supercomplex can be isolated from thylakoids solubilized with nonionic detergents under moderate conditions (*15*). Figure 1A shows the separation profile of the chlorophyll−protein complexes. The thylakoids purified from wild-type cells were solubilized with 0.8% DM, and the resulting extracts were separated by sucrose density gradient centrifugation. The gradient was collected from the bottom, and the fractionation profile was monitored by measuring the absorption at 670 nm. Three major peaks were clearly detected (A-1, A-2, and A-3 from the top of the gradient). Western blotting using anti-PsaD antibody indicates that most of the PSI is present in A-3 (fractions 6−8), and a small amount of PSI is in A-2 (fractions 9 and 10). PSII was exclusively present in A-2, while LHCII was separated in A-1 as described in refs *15* and *18*. Western blotting using LHCI antibodies (anti-p14.1, p15, and p18.1) revealed that the separation profile of LHCI is almost identical to that of PSI, indicating that LHCI is copurified with PSI on the sucrose density gradient. Two signals in A-1 (fractions 11−15), which were visualized with anti-p15, are ascribed to its cross-reaction to LHCII proteins.

Fraction A-3 was subsequently loaded onto a DEAE column and separated with a buffer containing a linear gradient of NaCl (Figure 1B). We identified a single peak containing both PSI and LHCI proteins, indicating that the PSI and LHCI are stably associated to form a homogeneous PSI−LHCI supercomplex. In addition, this chromatographical purification step improved the fluorescence emission spectrum at 77 K; a shoulder peak at 685 nm, which may be ascribed to a small contamination of the LHCII and/or PSII, was almost removed (data not shown). The chlorophyll a/b ratio was estimated to be 5.1, which is consistent with the reported value of 4.4−5.1 (*3*, *6*).

Purification of LHCI from Δpsa B Cells. The LHCI is synthesized normally and stably accumulated in the absence of the PSI core complexes (*10*). The *C. reinhardtii* LHCI consists of several distinctive polypeptides (*3*, *11*), and as shown in Figure 1, all of the LHCI polypeptides detected in the present study are associated with the PSI complex. We compared the polypeptide compositions of the wild-type PSI−LHCI supercomplex and the LHCI from the PSI-deficient mutant Δ*psaB* (*19*). Thylakoids from Δ*psaB* cells were solubilized under the same conditions as wild-type thylakoids and were separated by sucrose density gradient

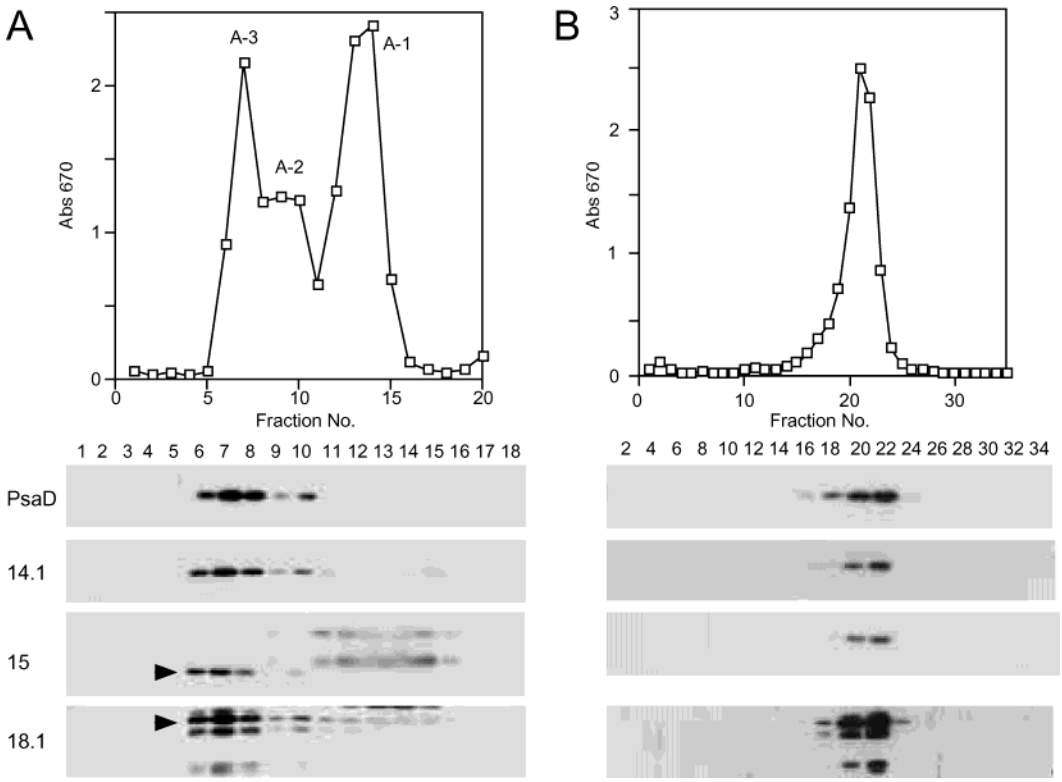

FIGURE 1: Purification of the PSI−LHCI supercomplex from wild-type cells. Thylakoids purified from wild-type cells (0.8 mg chl/mL) were solubilized with 0.8% DM and subsequently separated by sucrose density gradient centrifugation (A). The gradient was collected from the bottom to the top, and the fractionation profile was monitored by an absorption at 670 nm. The resulting fractions were analyzed by Western blotting using antibodies against PsaD and LHCI polypeptides (p14.1, p15, and p18.1). Anti-p15 and anti-p18.1 antibodies cross-reacted against other Lhca polypeptides; arrowheads indicate p15 and p18.1 bands. Fraction A-3, which is enriched in the PSI−LHCI supercomplex, was further purified by DEAE column chromatography (B). The fractions were eluted with a linear gradient of NaCl (25−150 mM) in 50 mM Tris-HCl at pH 8.0 and 0.05% DM, and they were monitored by an absorption at 670 nm. The collected fractions were analyzed by Western blotting using the same antibodies as in A.

centrifugation (Figure 2A). We found two major bands (A-1 and A-2) as well as a shoulder (A-3). Band A-1 contained the LHCII, while A-2 consisted of the PSII core complex. Western blotting using LHCI antibodies indicated that LHCI is present in A-3 (fractions 5−12). Because this mutant lacks PSI, A-3 was detected as a shoulder. The apparent molecular mass of the LHCI on the sucrose density gradient was estimated to be 300−400 kDa, indicating that the LHCI polypeptides form a large complex even in the absence of PSI. Of great interest is that the majority of the p14.1 (Lhca3) polypeptide was separated at a slightly higher position than the LHCII (fraction 16). Other LHCI polypeptides were not detected in this fraction. This indicates that most of the p14.1 polypeptide was present as a monomer in the thylakoids or was easily dissociated from the oligomeric form of LHCI during solubilization and purification. Whether this polypeptide still binds pigments is unknown.

Because A-3 was still contaminated by other polypeptides, we subjected this fraction to DEAE column chromatography to further purify the LHCI. The LHCII separated into fractions 2−16, which contained low concentrations of NaCl, and a small amount of LHCI eluted into factions 8−18 (Figure 2B). The main portion of LHCI eluted at approximately 100 mM NaCl (fractions 24−30). In these fractions, Lhca3 remaining in the LHCI-enriched fraction copurified with other LHCI polypeptides. The third peak, eluting at a higher concentration of NaCl, contained the PSII complex. These observations indicate that the DEAE column chromatography effectively removed the contaminating LHCII and PSII complex from the LHCI (Figure 2B). The chlorophyll a/b ratio of the purified LHCI was estimated to be 2.7, which is more similar to the ratio of 2.8 in LHCI-705 than 2.1 in LHCI-680 (*3*).

More severe treatment of the PSI−LHCI supercomplex generates two types of LHCI, LHCI-680 and LHCI-705 (3). However, one main type of LHCI was isolated from the PSI-deficient mutant (Figure 2). Fluorescence emission spectrum measured at 77 K showed a peak at 708 nm and a shoulder at 685 nm, reminiscent of those of LHCI-705 and LHCI-680, respectively (Figure 3). The fluorescence peaking at 708 nm may correspond to a typical emission band from an oligomeric form of LHCI, and the fluorescence at 685 nm might be derived from a more modified form of LHCI (*3*). This suggests that, during the purification process, there is a small modification to the structural integrity of the purified LHCI.

We next compared the polypeptide profile of the PSI−LHCI and LHCI preparations. The left panel in Figure 4 shows the polypeptides separated on the SDS−polyacrylamide gel, which has an improved resolution in the 20−30-kDa range (*15*, *16*). In addition to PsaD and PsaF in the PSI−LHCI supercomplex, this gel resolved at least seven polypeptide bands (a−g). Band e appeared as a diffuse band migrating above f, and re-electrophoresis of the excised gel containing bands e and f clearly showed two distinct bands. These bands from a to g are assigned as Lhca4 (p14), Lhca6 (p18.1), Lhca3 (p14.1), Lhca5 (p15.1), Lhca7 (p15), Lhca8 (p18), and Lhca1 (p22.1), respectively (Table 1) (*20*).

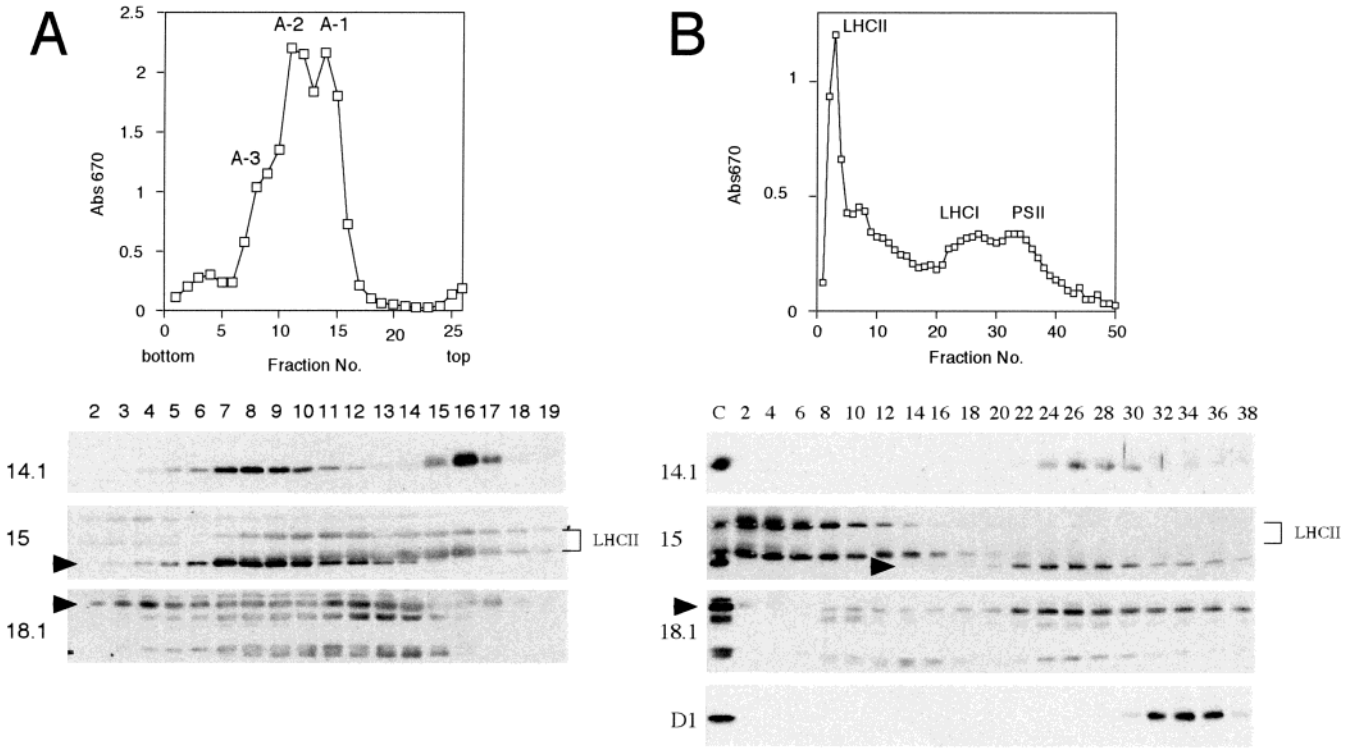

FIGURE 2: Separation of the LHCI from Δ*psaB* cells. Thylakoids purified from the Δ*psaB* cells (0.8 mg chl/mL) were solubilized with 0.8% DM and subsequently separated by sucrose density gradient centrifugation as described in Figure 1A. The gradient was collected from the bottom to the top, and the fractionation profile was monitored by an absorption at 670 nm. The resulting fractions were analyzed by Western blotting using antibodies against PsaD and LHCI polypeptides (p14.1, p15, and p18.1). Anti-p15 and anti-p18.1 antibodies cross-reacted against other Lhca polypeptides; arrowheads indicate p15 and p18.1 bands (A). Fraction A-3, which is enriched in LHCI, was further purified by DEAE column chromatography (B). The fractions were eluted with a linear gradient of NaCl concentration (25−175 mM) in 50 mM Tris-HCl at pH 8.0 and 0.05% DM, and they were monitored by an absorption at 670 nm. The collected fractions were analyzed by Western blotting using the same antibodies as in A.

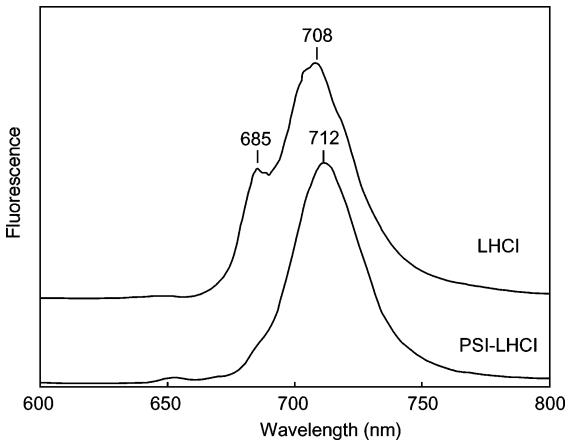

FIGURE 3: Fluorescence emission spectra of the PSI−LHCI supercomplex and LHCI at 77 K. These complexes were purified as described in Figures 1B and 2B, suspended in 50 mM Tris-HCl at pH 8.0 and 0.05% DM, and excited with an actinic light at 430 nm.

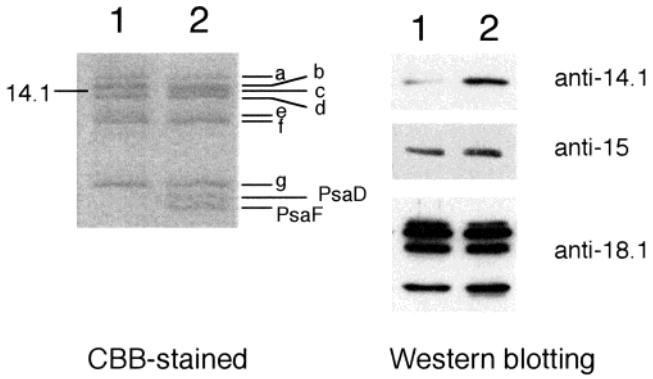

FIGURE 4: Comparison of the polypeptide profiles from wild-type and Δ*psaB* mutant strains. The purified LHCI from Δ*psaB* mutant cells (1) and the PSI−LHCI supercomplex from wild-type cells (2) are shown. Although seven distinctive Lhca polypeptides (a−g) were observed in the PSI−LHCI supercomplex, band c appears to be missing from the LHCI. Western blot analysis revealed that Lhca3 is significantly reduced in the LHCI.

Furthermore, as expected, neither PsaD nor PsaF was detected in LHCI from the Δ*psaB* strain, and band c, corresponding to Lhca3 (p14.1), was deficient or significantly reduced on the gel. This one-dimensional SDS−PAGE did not reveal any other differences between these two preparations. This was confirmed by the fact that Western blotting showed that p15 and p18.1, as well as several anti-p18.1 cross-reacting bands, which may correspond to bands a−f, were at essentially equal levels in the PSI−LHCI and LHCI preparations. However, as expected from the results in Figure 2, the amount of Lhca3 was significantly reduced in the LHCI but fully present in the PSI−LHCI supercomplex.

To determine in more detail which Lhca polypeptides are tightly associated with the PSI−LHCI supercomplex, we separated the polypeptides by 2DE and stained the gel with silver (Figure 5). To identify the Lhca polypeptides that do not copurify with the complex in the absence of PSI, the polypeptides of the LHCI isolated from Δ*psaB* were independently separated by 2DE, and the protein map was compared to the protein map from the PSI−LHCI supercomplex. Recent investigations of detergent-solubilized PSI−

Table 1: Genes of LHCI Polypeptides in *C. reinhardtii*

gene	protein	band on the gel
Lhca1	p22.1	g
Lhca2	p19	minor polypeptide
Lhca3	p14.1	c
Lhca4	p14	a
Lhca5	P15.1	d
Lhca6	p18.1	b
Lhca7	p15	e
Lhca8	p18	f
Lhca9	p22.2	minor polypeptide

LHCI supercomplex using 2DE coupled to Western blotting and MS/MS analysis (*11*, *17*) have identified the Lhca polypeptides present in individual 2DE spots and have shown that 2DE coordinates are reliable parameters for assigning protein identity. We therefore used these detailed 2DE maps for our current studies. In some cases, the identity of proteins in 2DE spots was confirmed by MS/MS analysis of tryptic peptides coupled with database searching (Table 2). In all cases, these results in Figure 5 confirmed previous analyses (*11*, *17*).

Comparison of the 2DE maps from PSI−LHCI and LHCI revealed that protein spots containing Lhca1 (p22.1; spots 2 and 29), Lhca7 (p15; spots 3, 4, 6−8, and 26), and Lhca8 (p18; spots 25 and 31) are enriched in the LHCI (Figure 5). In particular, spot 2, which is primarily composed of Lhca1 (p22.1), is the most intensely stained spot among the LHCI polypeptides on the 2DE gel. Spots 25 and 26, which are composed of only Lhca7 (p15) and Lhca8 (p18), respectively, are also enriched in the 2DE gel of the LHCI. In contrast to the spots containing the Lhca1, Lhca7, and Lhca8 proteins, the spots containing Lhca2 (p19; spot 8) and Lhca9 (p22.2; spot 1) are less intensely stained on the 2DE gel of the purified LHCI compared to those of the PSI−LHCI supercomplex. Spot 1, which is composed of only Lhca2-like polypeptide (p22.2), and spot 8, which is primarily composed of Lhca2 (p19), are present on the 2DE map of the Δ*psaB* thylakoids (see open circles in Figure 5a) and on the 2DE map of the PSI−LHCI supercomplex but not on the 2DE map of the LHCI (Figure 5). This indicates that these proteins are present in the thylakoid membrane but do not associate stably with the LHCI in the absence of PSI.

Spot 34 was detected on the 2DE gel of the PSI−LHCI supercomplex but not on the 2DE gel of the LHCI. The MS/MS analysis indicates that this spot corresponds to the α subunit of cytochrome b_{559}. Although the PSI−LHCI supercomplex is highly purified by sucrose gradient centrifugation and DEAE chromatography, the presence of other thylakoid-membrane proteins in this fraction is not completely excluded. The presence of this PSII−RC polypeptide with the PSI−LHCI supercomplex is thus probably an artifact of the purification procedure.

The protein spots containing Lhca5 (p15.1; spots 6−10), Lhca6 (p18.1; spots 7 and 9−11), and Lhca4 (p14; spots 7 and 33) are, for the most part, less intensely stained on the 2DE gel of the LHCI, although p14 (spot 33) may be slightly enriched in the LHCI. These Lhca polypeptides constitute minor components of the purified LHCI. In addition, Lhca3 (p14.1) is less abundant in the LHCI than in the PSI−LHCI supercomplex when the spot volumes were analyzed by Phoretix 2D software. This agrees with the immunoblots and the SDS−PAGE analyses (Figure 3).

Interestingly, a new protein spot appears on the 2DE gel of the purified LHCI (Figure 5). This 2DE spot is induced in thylakoids isolated from *C. reinhardtii* grown in iron-deficient media and was identified as an Lhca protein by Western blotting (*21*). Analysis of this 2DE spot with MS/MS suggests that this polypeptide is an N-terminal-processed form of Lhca3 (Stauber, E. J. and Hippler, M., unpublished). This is not surprising because Lhca3 is expected to be more susceptible to proteolytic degradation in the absence of PSI.

DISCUSSION

In the present paper, we used sucrose density gradient centrifugation and DEAE column chromatography to purify the PSI−LHCI supercomplex from wild-type *C. reinhardtii* and the LHCI the PSI-deficient *C. reinhardtii* mutant Δ*psaB*, and we compared the polypeptide composition of the two complexes. Relatively strong solubilization treatments are required for dissociation of LHCI from wild-type cells because of the tight association between the PSI core and LHCI. As a result, two types of LHCI, LHCI-680 and LHCI-705, are separated from wild-type *C. reinhardtii* (*3*). Although these LHCI subfractions emitted different low-temperature fluorescence emission maxima, the polypeptide composition was not distinguishable. Because the LHCI is synthesized normally in the PSI-deficient Δ*psaB* cells (*10*) but is not associated with the PSI complexes, it was easily purified under mild conditions. In addition, only one main type of LHCI was isolated from the mutant cells, probably as a result of these mild conditions, and we suggest that the two types of LHCI isolated in the former study correspond to different aggregation states caused by the detergent treatment (*3*). Thus, it appears that the LHCI isolated from the Δ*psaB* mutant maintains its structural and functional features to a higher extent than the complex isolated from the wild-type cells. Finally, on the basis of the apparent molecular mass of the LHCI on sucrose density gradients, we can conclude that the core of the LHCI from *C. reinhardtii* forms a stable multiprotein complex that is different from the apparent dimeric structures of LHCI from vascular plants.

The comparative analyses of the polypeptide composition of the PSI−LHCI supercomplex and the LHCI provided for us some new insight into the subunit structure of LHCI in *C. reinhardtii*. Western blotting of fractions from sucrose density gradients and DEAE column chromatography revealed that almost all of the Lhca polypeptides copurified with PSI polypeptides. The one-dimensional SDS−PAGE system optimized for separation of Lhca polypeptides resolved seven distinct polypeptides (corresponding to a−g) from the PSI−LHCI supercomplex (Figure 4). In addition, the 2DE system showed highly detailed polypeptide profiles of Lhca polypeptides as reported previously (*11*, *17*). The immunochemical results showed that most of Lhca3 (p14.1) dissociated from the oligomeric LHCI from Δ*psaB* cells, although this polypeptide was tightly associated with the PSI−LHCI supercomplex. Thus, the purified LHCI from the mutant contained a significantly reduced amount of Lhca3 (p14.1) (Figure 3). The 2D protein maps of the PSI−LHCI supercomplex and the LHCI indicated that, in the LHCI compared to the PSI−LHCI supercomplex, Lhca1 (p22.1), Lhca7 (p15), and Lhca8 (p18) are enriched, whereas Lhca2 (p19), Lhca3 (p14.1), and Lhca9 (p22.2) are diminished. This

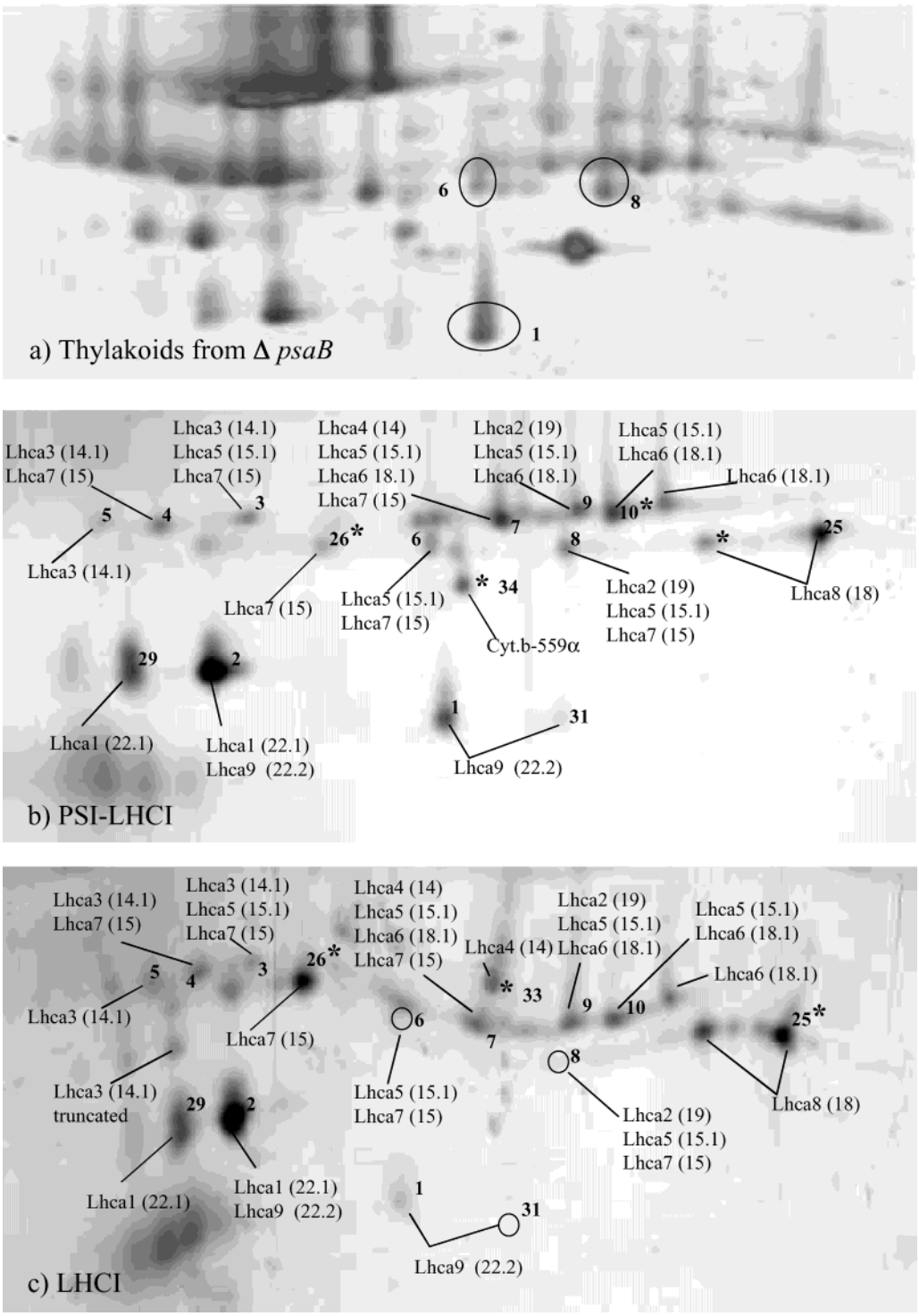

FIGURE 5: 2DE analysis of Lhca polypeptides. The thylakoids proteins from Δ*psaB* cells (a), PSI−LHCI supercomplex from wild-type cells (b), and LHCI from Δ*psaB* cells (c) were visualized by silver staining. The identity of the protein spots and labeling of Lhca polypeptides was inferred from the previous 2DE analysis of PSI particles or MS/MS analysis of thylakoids (*11*). Spots that were reanalyzed by MS/MS are indicated with an asterisk. Open circles in panel c show polypeptide spots that are lacking in the LHCI for the Δ*psaB* mutant but are present in the PSI−LHCI supercomplex for wild-type cells. Analysis of spot volumes from LHCI and PSI−LHCI maps resulted in the following ratios for PSI−LHCI/LHCI spots: 1:10.5, 2:0.85, 3:3.6, 4:2.3, 8:8.3, 9:0.9, 25:0.6, 26:0.2, and 29:0.8. Analysis of the spots was done using Phoretix 2D version 2004 (Build 1440.1) software using automatic spot picking and default values.

suggests that a majority of the Lhca2 (p19), Lhca3 (p14.1), and Lhca9 (p22.2) polypeptides in the thylakoids are weakly associated with the oligomeric LHCI or remain as a monomer. In either case, the presence of the PSI core complex is required for the stable binding of these three polypeptides to the LHCI. In addition, we propose that Lhca polypeptides, Lhca1 (p22.1), Lhca7 (p15), and Lhca8 (p18), together with the minor polypeptides, Lhca4 (p14) and Lhca6 (p18.1), form a stable multiprotein complex independent of the assembly of the PSI core complex in the thylakoid membrane.

The three-dimensional structure of the PSI−LHCI supercomplex from green plants has been recently examined by electron microscopy. This analysis indicates that, in contrast

Table 2: MS/MS Data for Selected Silver-Stained Spots[a]

complex	spot	protein	peptide	position	z	ΔM	X_{corr}
LHCI	25	Lhca8	YATGAGPVDNLAAHLK	211−226	2	0.7	4.21
		Lhca8	WYQQAELIHC[+57]R	68−78	2	1.0	3.39
		Lhca8	AGALNVPEWYDAGK	96−109	2	0.8	2.79
	26	Lhca7	NPGSQADGSFLGFtEEFK	141−158	2	1.1	5.52
		Lhca7	FFDPMGLSR	169−171	2	1.0	3.11
	33	Lhca4	WYAQAELMNAR	95−105	2	1.4	2.99
PSI−LHCI	10	Lhca5	NFGSVNEDPIFK	142−253	2	0.3	4.09
		Lhca5	LWAPGVVAPEYLK	34−46	2	−1.7	3.30
	25	Lhca8	TAMAGVAGILIPGLLTK	79−95	2	−0.2	3.24
		Lhca8	GTSELGYPGGPFDPLGLSK	162−180	2	0.8	3.18
		Lhca8	WYQQAELIHC[+57]R	68−78	2	−0.3	2.55
	26	Lhca7	VGLGFPEWYDAGK	95−107	2	−0.4	3.26
	34	Cytb559	PFSDILTSIR	8−17	2	1.0	3.59
		Cytb559	FNALEQVK	70−77	1	0.6	1.64

[a] The charge state (z) of the measured ion, as well as the calculated deviation (ΔM) of the experimentally determined mass from the theoretical average mass of the peptide, is given. The position of the peptide within the preprotein sequence is listed. Carbamidomethylation of cysteine (57 Da) residues is indicated where necessary. The cross-correlation factor (X_{corr}) calculated by the Sequest algorithm is listed in the far right column. All peptide sequences reported produced cross-correlation factors equal to or above 1.5, 2.25, or 3.5 for single-, double-, and triple-charged precursor ions, respectively.

to the trimeric form of the PSI core complex in cyanobacteria, the PSI−LHCI supercomplex of green plants is a monomer and that LHCI complexes consisting of 8−14 Lhca polypeptides form a half-ring structure that binds to one side of the PSI core complex (*6*, *7*). It appears that the oligomeric structure of the LHCI is located close to PsaK, PsaJ, PsaF, and PsaG, which possess one or more transmembrane helices, but is not close to PsaL, which is required for trimerization of the PSI core complex in cyanobacteria (*22*). Indeed, in agreement with the proposed structural model, interactions between PsaK and the LHCI as well as between PsaK/PsaG and the LHCI have been reported (*23*, *24*). However, how distinct Lhca polypeptides are organized into the oligomeric form of the LHCI is not currently clear. The proposed model also suggests that eight Lhca polypeptides form four dimers, while three additional Lhca polypeptides are monomers in the oligomeric LHCI structure (*7*). This heterogeneous localization of the Lhca polypeptides suggests different functions of each Lhca polypeptide in the oligomeric LHCI.

Recent determination of the crystal structure of the PSI−LHCI supercomplex from a higher plant has revealed that the LHCI of 150 kDa consists of only four Lhca polypeptides (*9*). In contrast, the LHCI from *C. reinhardtii* consists of seven major Lhca polypeptides, and its size was estimated to be 300−400 kDa. In fact, the particle size of the PSI−LHCI supercomplex from *C. reinhardtii* estimated by electron microscopy and image analysis is significantly larger than that of a higher plant (*6*).

Although the LHCI purified from Δ*psaB* cells forms an oligomeric structure, it is not known whether it retains the half-ring structure in the absence of the PSI core complex. The remarkable decrease in Lhca2, Lhca3, and Lhca9 in the purified LHCI indicates that there is no significant involvement of these three polypeptides in the oligomerization of the other Lhca polypeptides. This suggests that these three Lhca polypeptides might be located in an interface between the oligomeric structure of the LHCI and the PSI core complex and that their association with the LHCI is stabilized by the presence of the PSI core complex. This intimate structural interaction between these Lhca polypeptides and the PSI core complex may suggest a functional role in the transfer of light energy absorbed by the LHCI to the PSI core complex. Lhca3 (p14.1) and Lhca1 (p22.1) are relatively well-conserved in *C. reinhardtii* and higher plants and are classified as type III and type I proteins, respectively, according to phylogenic analyses (*25*). These two polypeptides are reminiscent of the minor light-harvesting complexes of PSII, CP24, CP26, and CP29, which are located between the PSII core complex and the major LHCII. These three complexes are involved in excitation energy transfer from the major LHCII to the PSII core complex. Interestingly, except for Lhca1 and Lhca3, the Lhca proteins are rather variable among green algae and higher plants. Together, Lhca3, as well as Lhca2, Lhca9, and probably Lhca1, could be directly bound to the PSI core complex and thus could participate in transferring excitation energy from a more peripheral LHCI consisting of Lhca4, Lhca5, Lhca6, Lhca7, and Lhca8 to the PSI core complex.

In conclusion, our results support the concept that, for the PSI−LHCI supercomplex of *C. reinhardtii*, the PSI complex and LHCI first assemble independently and then integrate into the thylakoid membrane (*26*). The integration of the two complexes appears to allow the stable association of the Lhca2, Lhca3, and Lhca9 polypeptides to the LHCI. In addition, the biochemical properties suggest that the LHCI of *C. reinhardtii* is approximately two times larger than that of a higher plant.

ACKNOWLEDGMENT

Antibodies raised against D1 and PSI polypeptides were kindly provided by Drs. M. Ikeuchi (University of Tokyo) and J.-D. Rochaix (University of Geneva), respectively. The *psaB*-deficient mutant strain was kindly provided by Dr. K. Redding (University of Alabama).

REFERENCES

1. Mullet, J. E., Burke, J. J., and Arntzen, C. J. (1980) Chlorophyll proteins of photosystem I, *Plant Physiol. 65*, 814−822.
2. Eshaghi, S., Andersson, B., and Barber, J. (1999) Isolation of a highly active PSII−LHCII supercomplex from thylakoid membranes by a direct method, *FEBS Lett. 446*, 23−26.
3. Bassi, R., Soen, S. Y., Frank, G., Zuber, H., and Rochaix, J. D. (1992) Characterization of chlorophyll a/b proteins of photosystem I from *Chlamydomonas reinhardtii*, *J. Biol. Chem. 267*, 25714−25721.

4. Lam, E., Ortiz, W., and Malkin, R. (1984) Chlorophyll a/b proteins of Photosystem I, *FEBS Lett. 168*, 10−14.
5. Boekema, E. J., Jensen, P. E., Schlodder, E., van Breemen, J. F., van Roon, H., Scheller, H. V., and Dekker, J. P. (2001) Green plant photosystem I binds light-harvesting complex I on one side of the complex, *Biochemistry 40*, 1029−1036.
6. Germano, M., Yakushevska, A. E., Keegstra, W., van Gorkom, H. J., Dekker, J. P., and Boekema, E. J. (2002) Supramolecular organization of photosystem I and light-harvesting complex I in *Chlamydomonas reinhardtii*, *FEBS Lett. 525*, 121−125.
7. Kargul, J., Nield, J., and Barber, J. (2003) Three-dimensional reconstruction of a light-harvesting complex I−photosystem I (LHCI−PSI) supercomplex from the green alga *Chlamydomonas reinhardtii*. Insights into light harvesting for PSI, *J. Biol. Chem. 278*, 16135−16141.
8. Castelletti, S., Morosinotto, T., Robert, B., Caffarri, S., Bassi, R., and Croce, R. (2003) Recombinant Lhca2 and Lhca3 subunits of the photosystem I antenna system, *Biochemistry 42*, 4226−4234.
9. Ben-Shem, A., Frolow, F., and Nelson, N. (2003) Crystal structure of plant photosystem I, *Nature 426*, 630−635.
10. Wollman, F. A., and Bennoun, P. (1982) A new chlorophyll−protein complex related to photosystem I in *Chlamydomonas reinhardtii*, *Biochim. Biophys. Acta 680*, 352−360.
11. Stauber, E. J., Fink, A., Markert, C., Kruse, O., Johanningmeier, U., and Hippler, M. (2003) Proteomics of *Chlamydomonas reinhardtii* Light-Harvesting Proteins, *Eukaryotic Cell 2*, 978−994.
12. Chua, N.-H., and Bennoun, P. (1975) Thylakoid Membrane Polypeptides of *Chlamydomonas reinhardtii*: Wild-Type and Mutant Strains Deficient in Photosystem II Reaction Center, *Proc. Natl. Acad. Soc. U.S.A. 72*, 2175−2179.
13. Takahashi, Y., Matsumoto, H., Goldschmidt-Clermont, M., and Rochaix, J. D. (1994) Directed disruption of the *Chlamydomonas* chloroplast psbK gene destabilizes the photosystem II reaction center complex, *Plant Mol. Biol. 24*, 779−788.
14. Porra, R. J., Thompson, W. A., and Kriedemann, P. E. (1989) Determination of accurate extinction coefficients and simultaneous equations for assaying chlorophylls a and b extracted with four different solvents: verification of the cocentration of chlorophyll standards by atomic absorption spectroscopy, *Biochim. Biophys. Acta 975*, 384−394.
15. Takahashi, Y., Goldschmidt-Clermont, M., Soen, S. Y., Franén, L. G., and Rochaix, J.-D. (1991) Directed chloroplast transformation in *Chlamydomonas reinhardtii*: insertional inactivation of the *psaC* gene encoding the iron sulfur protein destabilizes photosystem I, *EMBO J. 10*, 2033−2040.
16. Fling, S. P., and Gregerson, D. S. (1986) Peptide and protein molecular weight determination by electrophoresis using a high-molarity Tris buffer system without urea, *Anal Biochem. 155*, 83−88.
17. Hippler, M., Klein, J., Fink, A., Allinger, T., and Hoerth, P. (2001) Towards functional proteomics of membrane protein complexes: analysis of thylakoid membranes from *Chlamydomonas reinhardtii*, *Plant J. 28*, 595−606.
18. Sugimoto, I., and Takahashi, Y. (2003) Evidence that the PsbK polypeptide is associated with the photosystem II core antenna complex CP43, *J. Biol. Chem. 278*, 45004−45010.
19. Redding, K., MacMillan, F., Leibl, W., Brettel, K., Hanley, J., Rutherford, A. W., Breton, J., and Rochaix, J. D. (1998) A systematic survey of conserved histidines in the core subunits of Photosystem I by site-directed mutagenesis reveals the likely axial ligands of P700, *EMBO J. 17*, 50−60.
20. Tokutsu, R., Teramoto, H., Takahashi, Y., Ono, T. A., and Minagawa, J. (2004) The Light-Harvesting Complex of Photosystem I in *Chlamydomonas reinhardtii*: Protein Composition, Gene Structures and Phylogenic Implications, *Plant Cell Physiol. 45*, 138−145.
21. Moseley, J. L., Allinger, T., Herzog, S., Hoerth, P., Wehinger, E., Merchant, S., and Hippler, M. (2002) Adaptation to Fe-deficiency requires remodeling of the photosynthetic apparatus, *EMBO J. 21*, 6709−6720.
22. Zouni, A., Witt, H. T., Kern, J., Fromme, P., Krauss, N., Saenger, W., and Orth, P. (2001) Crystal structure of photosystem II from *Synechococcus elongatus* at 3.8-Å resolution, *Nature 409*, 739−743.
23. Jensen, P. E., Gilpin, M., Knoetzel, J., and Scheller, H. V. (2000) The PSI-K subunit of photosystem I is involved in the interaction between light-harvesting complex I and the photosystem I reaction center core, *J. Biol. Chem. 275*, 24701−24708.
24. Jensen, P. E., Rosgaard, L., Knoetzel, J., and Scheller, H. V. (2002) Photosystem I activity is increased in the absence of the PSI-G subunit, *J. Biol. Chem. 277*, 2798−2803.
25. Teramoto, H., Ono, T., and Minagawa, J. (2001) Identification of Lhcb gene family encoding the light-harvesting chlorophyll-a/b proteins of photosystem II in *Chlamydomonas reinhardtii*, *Plant Cell Physiol. 42*, 849−856.
26. Hippler, M., Rimbault, B., and Takahashi, Y. (2002) Photosynthetic complexc assembly in C*hlamydomonas reinhardtii*, *Protistologica 153*, 197−220.

BI035988Z